

Article

Optimal Capacity and Cost Analysis of Battery Energy Storage System in Standalone Microgrid Considering Battery Lifetime

Pinit Wongdet¹, Terapong Boonraksa², Promphak Boonraksa³, Watcharakorn Pinthurat⁴ ,
Boonruang Marungsri^{1,*}  and Branislav Hredzak^{4,*}

¹ School of Electrical Engineering, Suranaree University of Technology, Nakhon Ratchasima 30000, Thailand

² School of Electrical Engineering, Rajamangala University of Technology Rattanakosin, Nakhon Pathom 73170, Thailand

³ School of Electrical Engineering, Faculty of Engineering and Architecture, Rajamangala University of Technology Suvarnabhumi, Nonthaburi 11000, Thailand

⁴ School of Electrical Engineering and Telecommunications, The University of New South Wales, Sydney 2052, Australia

* Correspondence: bmsvhee@sut.ac.th (B.M.); b.hredzak@unsw.edu.au (B.H.)

Abstract: In standalone microgrids, the Battery Energy Storage System (BESS) is a popular energy storage technology. Because of renewable energy generation sources such as PV and Wind Turbine (WT), the output power of a microgrid varies greatly, which can reduce the BESS lifetime. Because the BESS has a limited lifespan and is the most expensive component in a microgrid, frequent replacement significantly increases a project's operating costs. This paper proposes a capacity optimization method as well as a cost analysis that takes the BESS lifetime into account. The weighted Wh throughput method is used in this paper to estimate the BESS lifetime. Furthermore, the well-known Particle Swarm Optimization (PSO) algorithm is employed to maximize battery capacity while minimizing the total net present value. According to simulation results, the optimal adjusting factor of 1.761 yields the lowest total net present value of US\$200,653. The optimal capacity of the BESS can significantly reduce the net present value of total operation costs throughout the project by extending its lifetime. When applied to larger power systems, the proposed strategy can further reduce total costs.

Keywords: standalone microgrid; renewable energy; battery lifetime; capacity optimization; PSO algorithm



Citation: Wongdet, P.; Boonraksa, T.; Boonraksa, P.; Pinthurat, W.; Marungsri, B.; Hredzak, B. Optimal Capacity and Cost Analysis of Battery Energy Storage System in Standalone Microgrid Considering Battery Lifetime. *Batteries* **2023**, *9*, 76. <https://doi.org/10.3390/batteries9020076>

Academic Editor: King Jet Tseng

Received: 30 November 2022

Revised: 18 January 2023

Accepted: 22 January 2023

Published: 23 January 2023



Copyright: © 2023 by the authors. Licensee MDPI, Basel, Switzerland. This article is an open access article distributed under the terms and conditions of the Creative Commons Attribution (CC BY) license (<https://creativecommons.org/licenses/by/4.0/>).

1. Introduction

Recently, Renewable Energy Resources (RESs) have become attractive sources in the electrical power system due to various advantages, such as being sustainable sources and being environmentally friendly [1,2]. The primary RESs are solar and wind energy generation sources. However, power generation from the RESs is intermittent because of its behavior. Therefore, renewable energy generation sources cannot be directly connected to the existing system or used without the appropriate management system [3,4]. A microgrid is a small power system constructed to manage Distributed Generators (DGs) from renewable energy and load clusters. The microgrid that connects to the bulk power system is called to be in “on-grid mode”, and when it disconnects from the bulk power system in an emergency, it is called to be in “islanded mode”. The microgrid that operates in the islanded mode can be called a standalone microgrid [5,6]. The standalone microgrid is common in remote or rural areas. Thus, the standalone microgrid's stability is low due to the lack of assistance from the bulk power system. The primary goal in the microgrid is to balance the power load and power generation without interrupting the load. Hence, it is necessary to have manageable power generation sources, such as diesel engine generators or the BESS, to control the microgrid's power [7,8]. A standalone microgrid consisting of renewable energy generation sources, load clusters, and BESS is widely used [9] and avoids

using diesel generators for environmental reasons. One of the significant problems for BESS applications is finding optimal capacity that considers the lifetime of BESS. Because of the high cost of the BESS, BESSs with a short life have been widely used in a microgrid. The performance assessment of the grid is primarily based on cost and reliability related to the system's lower greenhouse gas emissions [10]. The optimal size of PV and BESS in a microgrid for maintaining the longest BESS lifetime using the Loss of Power Supply Probability (LPSP) and only the initial cost as the indicators was presented in [11]. The cost reduction analysis was estimated for the battery State of Health (SOH) and artificial intelligence was applied to help with the battery management system. A proper battery health assessment can extend the battery's lifetime and reduce the cost of the battery [12]. An accurate SOH is essential to optimizing battery lifespan. Battery deterioration tracking and SOH estimates are based on electrochemical impedance spectroscopy and the distribution of relaxation time measurements. They were used to look for indicators linked to deterioration [13]. The BESS lifetime estimation in a PV system using a practical model was presented by [14]. The authors also considered the impact of BESS sizes and types on its lifetime. The BESS lifetime increases with increased BESS size, and upfront costs also increase. The authors also introduced a strategy to optimise the total cost, including upfront costs and the replacement cost of BESS. The lifetime prediction method and sizing of lead-acid BESS in microgrids were applied by varying the BESS's size and the weighted Wh throughput method to estimate the BESS lifetime. However, the authors did not consider the cost analysis to obtain the optimal size [15]. This paper proposes an optimization of BESS on a microgrid with PV and WT as the power generation source. The objective function of this study is to reduce total costs. According to the literature review, the articles in the references [11,14] used a microgrid system with only PV and BESS. References [12,13] considered the SOH estimation method to reduce costs, but this paper uses the optimization method. The work in [14] only studied the BESS lifetime estimation in a PV system. Moreover, the authors in [15] did not consider the cost analysis to obtain the optimal size. Therefore, in this paper, both PV and WT generation systems are analyzed. The sizing and optimal NPV of the BESS were analyzed with the optimization method. Implementing a microgrid system requires forecasting investment costs and profits, as well as maintenance over its lifecycle because the batteries are expensive components of the microgrid system. If the battery is replaced prematurely, the cost of the system will increase. Forecasting and estimation methods are generally used for the life cycle and the replacement of the battery. However, this paper proposes optimization to get the best results and reduce the total cost of the BESS system. The weighted Wh method and the PSO algorithm are applied for optimizing the cost of BESS. In a standalone microgrid system, prolonging the life of the equipment is necessary to reduce the cost of its replacement. However, the size and installation costs of the storage systems must be appropriate. Therefore, this paper provides an appropriate weighting to minimize the cost of the microgrid system. The PSO algorithm is applied to determine the optimum weighting parameter, which results in faster and more accurate analysis results than statistical analysis.

The major contributions of the paper are summarized as follows: The capacity optimization method and cost analysis of the BESS by taking into account the BESS lifetime are proposed in this paper. The BESS lifetime is estimated using the weighted Wh throughput method, which is fully described in [16]. The total cost of the microgrid and the notion of Net Present Value (NPV) constructs serve as the objective function. The objective function is solved using the PSO algorithm to determine the BESS's ideal capacity. Due to its dependability and affordability, the lead-acid battery is used in this study. According to an economic analysis, it is a better choice than a modern battery like a lithium-ion battery [17,18].

The rest of this paper is structured as follows: Section 2 explains the mathematical modeling of DGs and BESS. Section 3 introduces the optimization model which consists of the objective function and the PSO algorithm. Section 4 provides the simulation results and result discussions. Finally, Section 5 concludes the paper.

2. DGs and BESS Models

In this section, the mathematical models of PV, WT and BESS used in the proposed optimization problem are briefly explained. A small industrial load is used for the case study in which PV and WT power generation systems are installed. The battery energy storage systems are used for power demand periods where the DGs are unable to supply the load for only some periods. Hence, BESS is small in size, and costs are reduced accordingly. However, the proper size of a BESS affects its longevity and maintenance or replacement costs. This model can be applied to the larger systems.

2.1. PV Model

The amount of PV power depends on the solar intensity and temperature and is given by [16],

$$P_{PV} = P_{STC} \cdot \frac{G_c}{G_{STC}} \cdot [1 + k(T_c - T_{STC})], \quad (1)$$

where P_{PV} is the output power; P_{STC} is the rated output power at standard conditions (the solar irradiance G_{STC} of 1000 W/m² and the temperature T_{STC} of 25 °C; G_c is the solar irradiance during operation; k is the discrete-time index and T_c is the temperature during operation. The installed capacity of the PV system in this paper is 65 kW_p.

2.2. Wind Turbine Model

The amount of generated WT power depends on the wind speed [19]. The output power of the WT system is expressed by,

$$P_{wt} = \begin{cases} 0, & v \leq v_{ci} \text{ OR } v \geq v_{co}, \\ P_{rated-wt} \frac{(v-v_{ci})}{(v_r-v_{ci})}, & v_{ci} \leq v \leq v_r, \\ P_{rated-wt}, & v_r \leq v \leq v_{co}, \end{cases} \quad (2)$$

where P_{WT} is the output power of the wind turbine; v is the wind speed and $P_{rated-wt}$ is the rated output power of WT. The capacity of the WT system is selected as 40 kW_p.

2.3. BESS Model

In this paper, a lead-acid battery is used for the calculation of the BESS cost because it is more cost-effective and safer compared to Li-ion battery. Although price of the Li-ion battery is continuing to decrease, it is still expensive in Thailand. In Thailand, the batteries widely used for energy storage in PV power generation systems are lead-acid batteries. In order to simulate the operation of the BESS, mathematical models for calculating the charge and discharge parameters and State of Charge (SOC) of the BESS are required. Batteries are bidirectional energy sources, meaning they can store energy in a manner comparable to an electrical load. In contrast, they provide energy as an energy source. The battery energy balance equation and its constraint are,

$$E_B(t + \Delta t) = E_B(t) + (P_{B,ch}(t) \cdot \eta_{B,ch} - P_{B,d}(t) / \eta_{B,d}) \Delta t, \quad (3)$$

$$E_B^{min} \leq E_B(t) \leq E_B^{max}, \quad (4)$$

where E_B is the energy of the BESS at time t ; $P_{B,ch}$, $P_{B,d}$ are the charging and discharging powers of BESS; $\eta_{B,ch}$, $\eta_{B,d}$ are the charging and discharging efficiency of BESS respectively.

The maximum permissible output power of the BESS is limited as,

$$-P_{B,ch}^{max} \leq P_b(t) \leq P_{B,d}^{max}, \quad (5)$$

where $P_{B,ch}^{max}$, $P_{B,d}^{max}$ are the maximum charging and discharging powers of BESS.

The battery SOC and DOD can be obtained as,

$$SOC(t) = \frac{E_B(t)}{E_{B,rated}}, \quad 0 \leq SOC(t) \leq 1, \quad (6)$$

$$DOD = 1 - SOC, \quad (7)$$

where SOC is the battery state of charge; E_B is the energy of BESS at time t ; $E_{B,rated}$ is the rated energy and DOD is the battery depth of discharge.

The $SOC = 1$ or 0 means that the battery is fully charged or completely discharged respectively. The SOC at time t can be expressed as,

$$SOC(t + \Delta t) = SOC(t) \cdot (1 - \beta) + \frac{E_B(t + \Delta t)}{E_{B,rated}}, \quad (8)$$

where β is the battery's self-discharge rate.

The battery SOC should be maintained within the specific ranges that depend on the type of the battery,

$$SOC^{min} \leq SOC(t) \leq SOC^{max}, \quad (9)$$

where SOC^{min} , SOC^{max} are the minimum and maximum limits of battery SOC.

2.4. BESS Capacity Model

BESS is used to maintain the microgrid's power balance. Thus, the required power of a BESS is the power mismatch between the load and the power generation. The balance between load and generation can be achieved through,

$$P_{B,required}(t) = P_L(t) - P_{WT}(t) - P_{PV}(t), \quad (10)$$

where $P_{B,required}$ is the BESS' required power; P_L is the load demand; P_{WT} is the output power of WT and P_{PV} is the output power of PV.

Taking into account the charging and discharging efficiencies, the BESS power and its rated power can be rewritten as follows: [20],

$$P_B(t) = \begin{cases} P_{B,required}(t) / \eta_{B,d}, & P_{B,required}(t) > 0, \\ P_{B,required}(t) \times \eta_{B,ch}, & P_{B,required}(t) < 0, \\ 0, & P_{B,required}(t) = 0, \end{cases} \quad (11)$$

$$P_{B,rated} = \max(|P_B(t)|), \quad (12)$$

where $P_{B,rated}$ is the BESS's rated power.

The required energy from BESS can be calculated as,

$$E_{B,required} = \max(E_B(t)) - \min(E_B(t)). \quad (13)$$

The SOC of BESS should be kept within a specific range. Therefore, the rated energy considering DOD limits is expressed by

$$E_{B,rated} = \frac{E_{B,required}}{DOD^{max} - DOD^{min}}, \quad (14)$$

where DOD^{max} , DOD^{min} are the DOD limits of the BESS.

In order to reduce the SOC level of the BESS, oversizing of the BESS is considered in this paper, as discussed in the next section. The oversized BESS does not have the same lifetime as an optimal size BESS [21,22]. BESS's non-optimal size also increases investment costs. An adjusting factor is used to obtain the BESS' oversized energy as,

$$E_{B,Orated} = E_{B,rated} \times q_B, \quad (15)$$

where $E_{B,Orated}$ is the BESS's oversized energy, $E_{B,rated}$ is the BESS' rated energy and q_B is the adjusting factor.

The adjusting factor q_B is equal to or greater than 1. As the size of the battery can affect the DOD range, it follows that a battery with a higher capacity will last longer under identical conditions. However, the cost of installation will rise. Consequently, the parameter that must be optimized in this paper is q_B . The optimal values will result in longer battery life and a reduction in total system costs.

2.5. BESS Lifetime Estimation

In this paper, a weighted Wh throughput method is used to calculate the lifetime of a lead-acid battery. This method has been employed by many researchers [15,23], as it can roughly estimate the battery lifetime by using the SOC as the most significant factor for battery lifetime. The battery has an overall throughput calculated from the manufacturer's datasheet, which usually provides the relationship between the Cycles to Failure (CTF) and the different DODs as shown in Figure 1. In this study, the employed battery is the Sun Xtender PVX-2580L model (12 V, 3.096 kWh) [24].

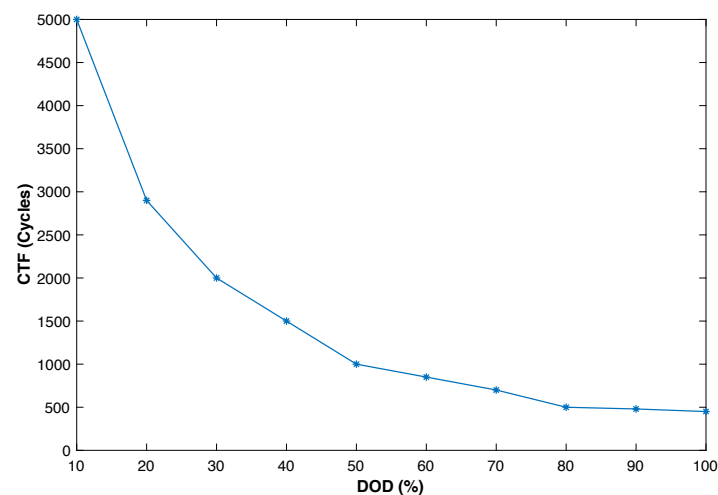


Figure 1. The relationship between CTF and DOD.

The energy throughput corresponding to a specific DOD is expressed as,

$$E_{throughput}(DOD) = 2 \times E_{B,rated} \times DOD \times CTF, \quad (16)$$

where $E_{throughput}$ is the energy throughput corresponding to a specific DOD and CTF is the cycles to failure.

Because the DOD varies within the range of DOD limits, the energy throughput varies with the DOD, as shown in Figure 2. By considering Equation (16) and the data shown in the Figure 1, the relationship between energy throughput and DOD in the Figure 2 can be obtained. The nonlinear curve in the Figure 2 is caused by the nonlinear function in the Figure which is the relationship between the Cycles to Failure (CTF) and different DODs. The data from the Figure 1 was obtained from the datasheet of the lead-acid battery in [24]. The overall energy throughput is the average energy throughput between the DOD limits and can be determined as,

$$E_{throughput,avg} = avg\{E_{throughput}(DOD)\}_{DOD(min)}^{DOD(max)}. \quad (17)$$

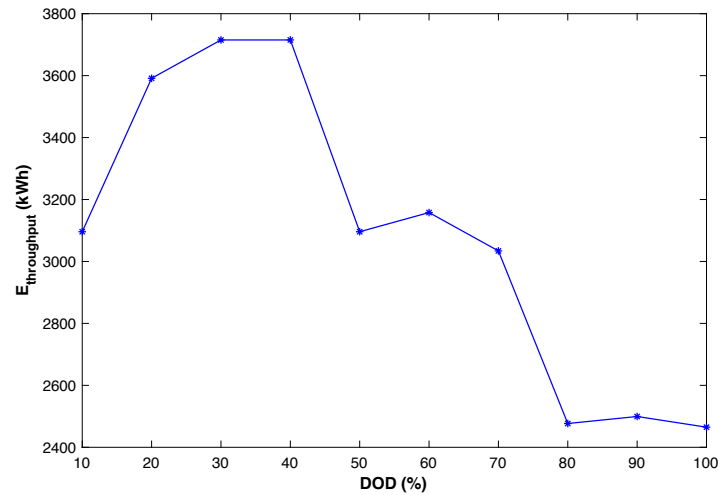


Figure 2. The relationship between energy throughput and DOD.

The cumulative energy throughput $E_{W_{SOC}}$ multiplied by the SOC weighting factor W_{SOC} during period Δt is given as,

$$E_{W_{SOC}} = W_{SOC} \times |P_B(t)| \times \Delta t. \quad (18)$$

The relationship between SOC and the weighting factor W_{SOC} is shown in Figure 3. For example, using 1 Wh of battery at 0.2 p.u. of SOC is equivalent to 1.3 Wh of the cumulative energy throughput. On the other hand, using 1 Wh at 1 p.u. of SOC is equal to 0.55 Wh of the cumulative throughput. Based on the Figure 3 that shows the relationship between SOC and SOC weighting factor and on Equations (18) and (19), battery life loss mainly depends on SOC and SOC weighting factor (SOC and W_{SOC}). If the SOC of the battery is kept lower, the battery life loss will be affected (see Equation (19)). Thus, the battery should operate at a high SOC or within its upper SOC limits to extend its lifetime. It has to be noted that this method ignores many influencing factors for simplicity, such as temperature, because temperature can be controlled. Therefore, the battery life loss can be calculated as,

$$L_{life} = \frac{E_{W_{SOC}}}{E_{throughput,avg}}, \quad (19)$$

where L_{life} is the battery life loss and $E_{throughput,avg}$ is the average energy throughput.

The battery is considered to reach the end of life when the total cumulative energy throughput is equal to the overall energy throughput.

The following exponential function can be used to express the relationship between the number of cycles and the depth of discharge,

$$N_{CTF} = f(DOD) = a \times e^{b \times DOD_B} + c \times e^{d \times DOD_B}, \quad (20)$$

where a, b, c, d are constants.

The depreciation (D_B) of BESS can then be calculated as,

$$D_B = \sum_{i=1}^m \frac{N_{B,cycle}(DOD_i)}{N_{CTF}(DOD_i)}, \quad (21)$$

where $N_{B,cycle}$ is the number of cycles according to the depth of discharge.

Therefore, the BESS lifetime L_B can be obtained as,

$$L_B = \frac{1}{D_{B,1year}} \times \text{years}, \quad (22)$$

where $D_{B,1year}$ is the depreciation of the battery in one year.

Hence, the total number of BESS replacements NR_B throughout the project is given by,

$$NR_B = \frac{L_p}{L_B} - 1. \tag{23}$$

where L_p is the project life.

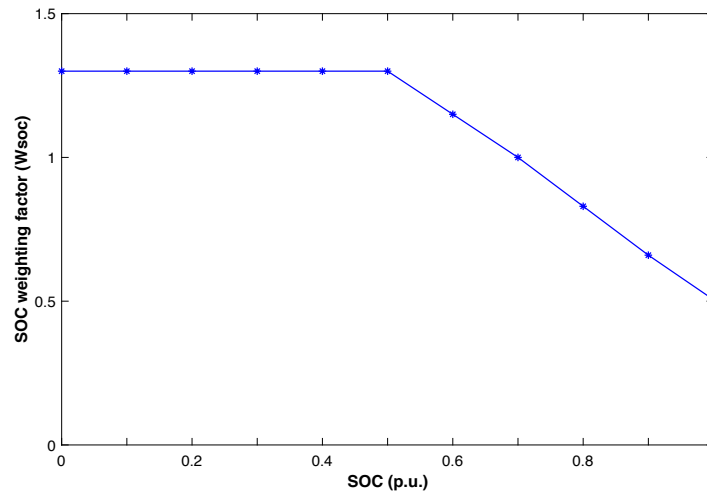


Figure 3. The relationship between SOC and the SOC weighting factor W_{SOC} .

3. Optimization Model

The optimization problem is introduced in this section, and the PSO algorithm used to solve it is briefly described.

3.1. Objective Function

The cost of the microgrid is represented by the concept of the Net Present Value (NPV). The total cost includes the initial cost, fixed operation and maintenance costs, and replacement costs. Therefore, the objective function used to minimize the NPV of the total cost can be defined as:

$$\text{Min}(NPVC_{total}) = \text{min}(C_{initial} + NPVC_{om} + NPVC_{re}), \tag{24}$$

where $NPVC_{total}$ represents the net present value of the total cost; $NPVC_{om}$ is the net present value of the fixed operation and maintenance costs; $NPVC_{re}$ is the net present value of the replacement cost and $C_{initial}$ is the initial cost.

The initial cost, the net present values of the replacement cost, and the fixed operation and maintenance costs respectively are given as,

$$C_{initial} = (k_{BE,initial} \times E_{B,Orated}) + (k_{BP,initial} \times P_{B,rated}), \tag{25}$$

$$NPVC_{re} = \sum_{n=1}^{NR_B} \frac{C_{initial}}{(1+d)^{NR_B \times L_B}}, \tag{26}$$

$$NPVC_{om} = k_{B,om} \times E_{B,Orated} \times USW, \tag{27}$$

where $k_{BE,initial}$ is the BESS initial cost per kWh (\$/kWh); $E_{B,Orated}$ is the BESS' oversized energy; $k_{BP,initial}$ is the BESS initial cost per kW (\$/kW); $k_{B,om}$ is the operation and maintenance costs set to 5% of the initial cost (\$/kWh/year); d is the discount rate (5%); L_B is the BESS lifetime and USW is the uniform series present worth factor.

The uniform series present worth factor is given as,

$$USW = \frac{(1 + d)^{L_p} - 1}{L_p(1 + d)^{L_p}}, \tag{28}$$

where d is the discount rate.

Figure 4 depicts the procedure flowchart for the BESS capacity determination. It starts by obtaining the input power of WT, PV, and load, and then calculating the rated power and energy capacity of the battery. Then, it estimates the BESS lifetime using the BESS model and obtains the objective function's value. If $NPVC_{total}$ is minimal, the calculation ends. If not, q_B is adjusted by incremental increases of 0.001 between 1 and 5 and the procedure is repeated.

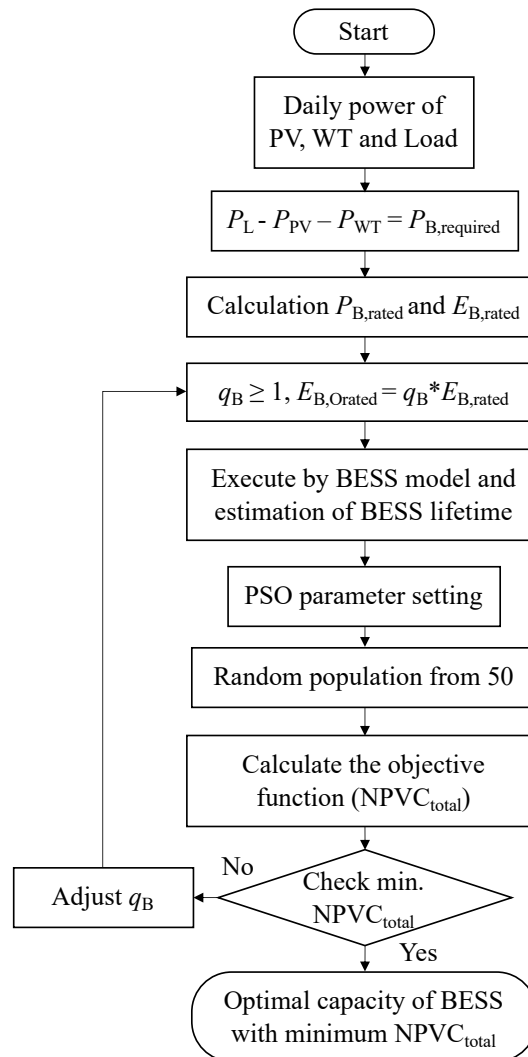


Figure 4. Flowchart for determination of the optimal BESS capacity. The q_B value is changed from 1 to 5 in 0.001 increments.

3.2. PSO Algorithm

Particle swarm optimization (PSO) is an intelligent optimization algorithm introduced by J. Kennedy and R. Eberhart [25]. It has been widely used in many works owing to its effectiveness and simplicity. The basics of PSO can be found in [26–28]. The reason for choosing the PSO algorithm is that it has a simple structure with few parameters and provides a quick solution. It creates particle swarms, which simulate a system or structure of a group of organisms that group together for some specific purpose in each organism.

The PSO chooses each i -th particle initial position and velocity at random. Then the i -th particle position and velocity are updated until the termination conditions are met. The particle's position and velocity of the particle i are expressed by,

$$x_i(k+1) = x_i(k) + v_i(k+1), \quad (29)$$

$$v_i(k+1) = w \times v_i(k) + c_1 r_{1i}(p_{i,best} - x_i(k)) + c_2 r_{2i}(g_{i,best} - x_i(k)), \quad (30)$$

where x_i is the position of particle i ; v_i is the velocity of the particle i ; w is the inertia factor; c_1, c_2 are the acceleration factors; r_1, r_2 are the random number [0–1]; p_{best} is the best particle and g_{best} is the best global solution.

Both acceleration factors (c_1, c_2) are commonly set to 2 [29]. The inertia factor which linearly decreases in each iteration ite is calculated as,

$$w_{ite} = w_{max} - ite \times \frac{w_{max} - w_{min}}{ite_{max}}, \quad (31)$$

where w_{max}, w_{min} are the weights of the maximum and minimum speeds and ite_{max} is the maximum iteration.

This paper applies the PSO algorithm to determine the optimal installation size of the BESS based on the battery size multiplier and the cost of the energy storage system throughout the project as a measure of fitness or sufficiency. Each particle in the herd has the battery size adjuster (q_B) as a variable and is assigned to represent the answer point. The initialization parameters for the PSO are the number of particles ($n = 50$), the maximum number of iterations ($ite_{max} = 100$), the range of velocity weighted values ($w_{max}/w_{min} = 0.9/0.4$), and the learning weighting value ($c_1, c_2 = 2$). The optimization toolbox in MATLAB is used to solve the PSO algorithm [30]. The effectiveness of the proposed strategy was verified using MATLAB running on MacBook Air (Early 2015), 1.6 GHz Dual-Core Intel Core i5, RAM 8 GB 1600 MHz DDR3. The verification findings for the suggested optimization approach are presented in the following section.

4. Results

In this study, a standalone microgrid with an industrial load, a WT, a PV and a BESS illustrated in Figure 5 is considered. The daily load demand, PV and WT generations with a 5-min resolution shown in Figure 6, tasken from [31], are used to verify the effectiveness of the proposed method. The industrial load has a peak power of 100 kW at 12:30 p.m. The PV generates power between 7:00 a.m. and 5:00 p.m. with a maximum value of 63 kW at noon. The power generated by wind turbines fluctuates around 35 kW throughout the day. The required power from the BESS is obtained based on the mismatch between the load demand and the total power generation. In Figure 7, the BESS' discharging power is positive and the charging power is negative. The initial SOC is set at 50%. The standalone microgrid project life is set to 20 years. The case parameters used in the optimization are given in Table 1.

Table 1. Case study parameters.

Parameter	Variable	Unit	Value
Project life	L_p	years	20
BESS Calendar life	L_B	years	10
BESS SOC limits	$SOC_{min} - SOC_{max}$	%	20–80
Charge/discharge efficiency	$\eta_{B,ch} / \eta_{B,d}$	%	90/90
Initial cost per energy [32–34]	$k_{BE,initial}$	\$/kWh	183.86
Initial cost per power	$k_{BP,initial}$	\$/kW	183.86
Operation & maintenance cost	$k_{B,om}$	\$/kWh/year	9.19
Discount rate [35]	d	%	5

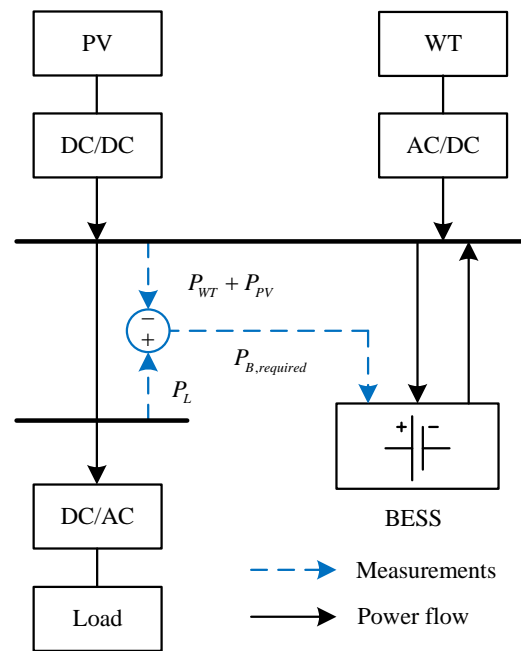


Figure 5. Schematic diagram of the standalone microgrid.

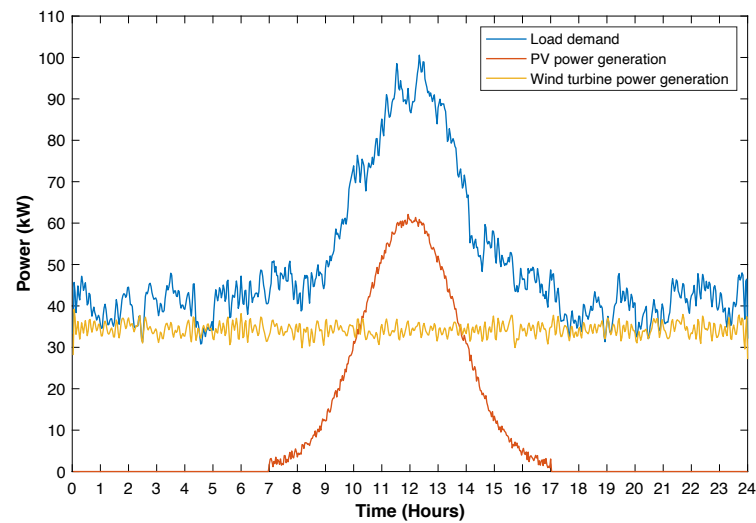


Figure 6. Industrial load, PV source and WT powers taken from [31].

The rated energy of BESS $E_{B,rated}$ is 82 kWh ($q_B = 1$). For $q_B = 1$, the BESS lifetime is 1.2 years, and the $NPVC_{total}$ throughout the project is US\$204,436. When $q_B = 1$, the SOC value is in the range of 20% to 80%. As the q_B is increased, the battery size is increasing, and the deviation of the battery SOC from 50% is decreasing. However, the increased battery capacity results in higher total costs. Thus, the PSO optimization method is applied to find the optimal value of q_B . The BESS SOC for $q_B = 1, 1.761, \text{ and } 5$ are illustrated in Figure 8.

Figure 9 shows a stepped pattern of the relationship between NR_B and q_B . As the q_B increases, the number of battery replacements will decrease. As the size of the battery increases, the SOH and the battery lifetime increase as well. The relationship between NR_B and L_B is shown as the purple line (saw-tooth pattern) and is used to obtain the $NPVC_{re}$ using Equation (26).

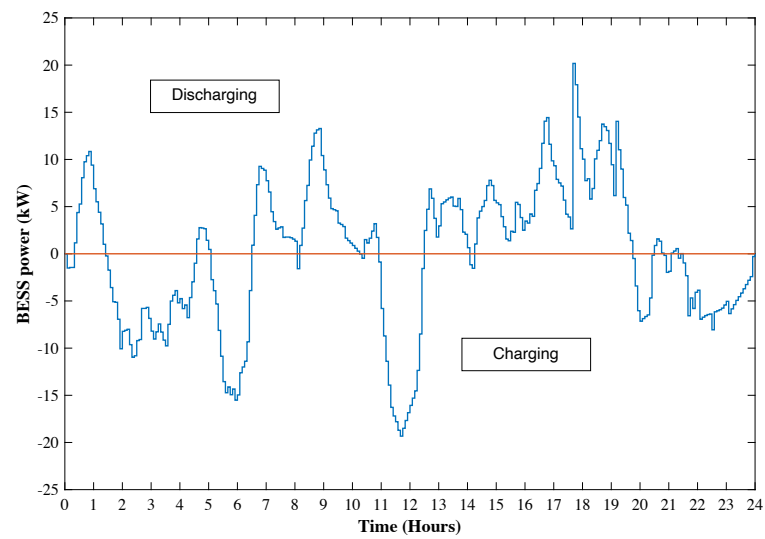


Figure 7. BESS–power for the case shown in Figure 6.

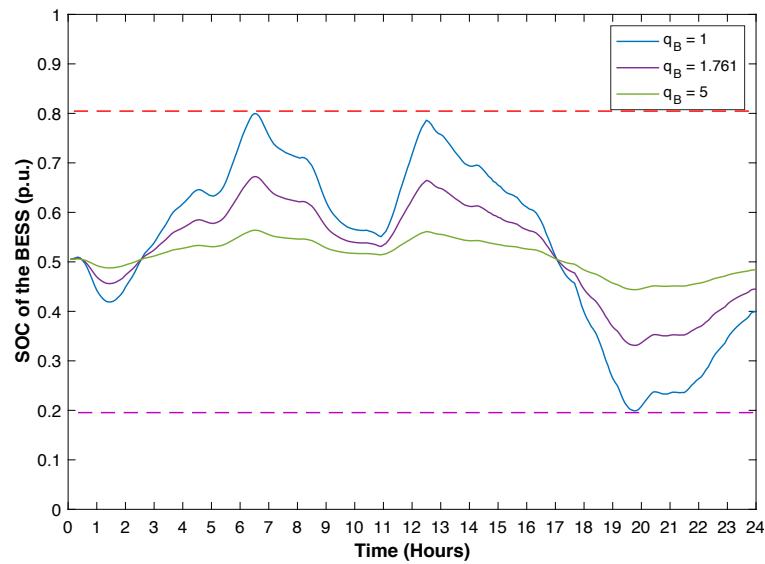


Figure 8. SOCs of BESS for q_B values of 1, 1.761 and 5.

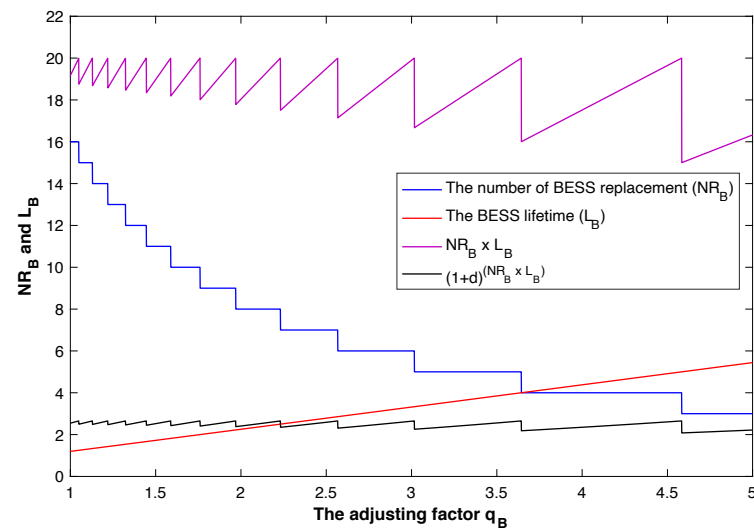


Figure 9. Relationships between NR_B and L_B for different values of q_B .

Using the proposed method, the obtained value of US\$200,653 was the lowest $NPVC_{total}$ at the q_B of 1.761. This corresponds to the optimal capacity of the BESS of 144.4 kWh. The effects of q_B on the $C_{initial}$, the $NPVC_{om}$ and the $NPVC_{re}$ are depicted in Figure 10. As the q_B increases, the size of the battery and the cost increase, and the number of replacements decreases. If the battery size is small, the cost of battery replacement is low, but the cost of replacing the battery is high. As the q_B varied from 1 to 5, in steps of 0.001, the $C_{initial}$ increased from US\$18,419 to US\$78,724, and the $NPVC_{om}$ increased from US\$23.48 to US\$117.43. In contrast, the C_{re} has downward trends because the q_B can extend the BESS lifetime and the BESS replacement was reduced.

The effects of q_B on the BESS lifetime and the number of BESS replacements are shown in Figure 11. The number of BESS replacements will decrease step by step with respect to the DOD and the size of the battery in relation to the q_B factor. However, when calculating the BESS replacement cost in the low q_B range, the replacement cost is low, and when q_B is high, the cost of replacing the battery increases. The minimum saw-tooth pattern range is the point where the number of BESS replacements is reduced. The q_B has a positive effect on the BESS lifetime. The BESS lifetime also increased from 1.2 years to 5.44 years when the q_B increased from 1 to 5. The number of BESS replacements decreased because the number of replacements remains equivalent even when q_B is adjusted slightly, such as when $NR_B = 8$ and $q_B = 2.0$ and 2.2.

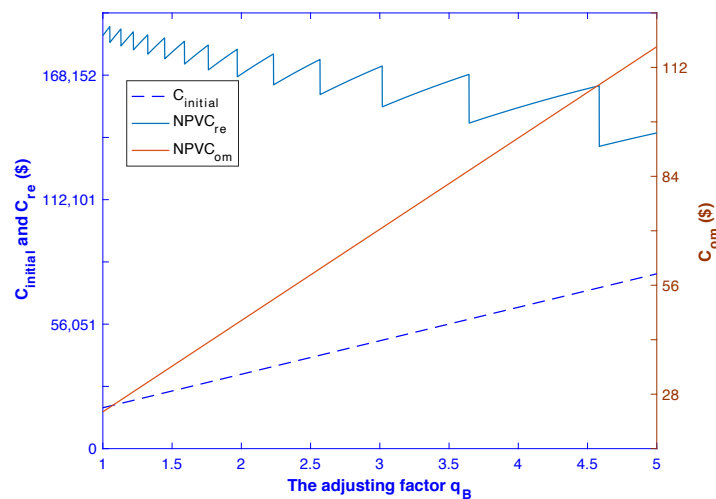


Figure 10. The costs for different values of q_B .

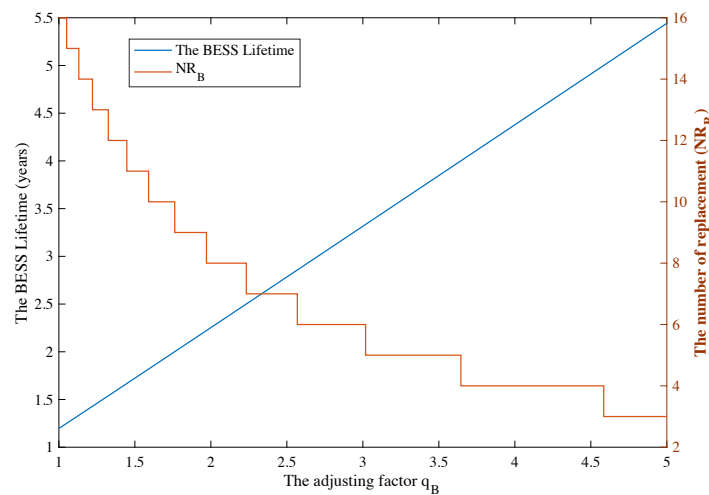


Figure 11. The BESS lifetime and the number of replacements for different values of q_B .

The q_B has an effect on the $NPVC_{total}$ of the microgrid, as shown in Figure 12. This curve is similar to a saw-tooth line due to the nonlinear characteristic of the replacement cost. When $q_B = 1.761$ and $q_B = 2.0$ are compared, the $NPVC_{total}$ of the $q_B = 1.761$ is the lowest. Even though the $C_{initial}$ and C_{om} for $q_B = 1.761$ are greater than those for $q_B = 2.0$, the C_{re} is lower because it can reduce the NR_B from 9 to 8. This shows how the q_B affects the $NPVC_{total}$. The BESS lifetime and cost analysis versus some of the q_B values are given in Table 2. Battery lifetime estimates show that increasing the size of the battery by the q_B factor increases battery life because it reduces the number of cycles at a high DOD value.

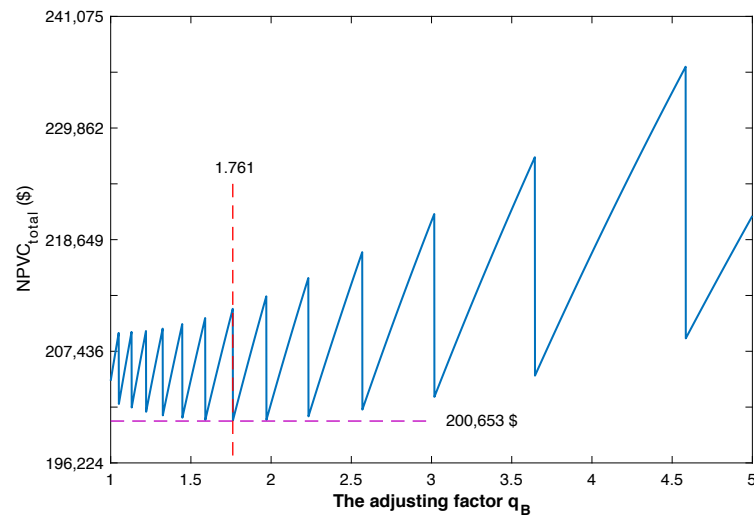


Figure 12. Net present value of the system total cost for different values of q_B .

Table 2. Simulation results for some of the q_B values.

q_B	L_B	NR_B	$C_{initial}$ (\$)	$NPVC_{om}$ (\$)	$NPVC_{re}$ (\$)	$NPVC_{total}$ (\$)
1.0	1.20	16	18,419	23.48	185,992	204,436
1.5	1.72	11	25,958	35.23	178,562	204,557
1.761	2.00	9	29,896	41.36	170,468	200,653
2.0	2.25	8	33,497	46.97	168,626	202,172
2.2	2.46	8	36,513	51.67	176,524	213,088
3.0	3.31	6	48,573	70.46	171,838	220,482
4.0	4.38	4	63,649	93.94	153,539	217,284
5.0	5.44	3	78,724	117.43	142,152	220,994

5. Conclusions

This paper proposed a capacity optimization method for a BESS in a standalone microgrid while taking the BESS' lifetime into account. The BESS' capacity influenced the initial cost, operation and maintenance costs, and replacement cost. The case study demonstrated the efficacy of the proposed method. According to the PSO algorithm results, the optimal capacity of the BESS ($q_B = 1.761$, $E_{B,rated} = 144.4$ kWh, and $NPVC_{total} = US\$200,653$) has the lowest NPV of the total cost. According to the simulation results, the capacity and lifetime of the BESS were the major factors influencing the total cost of the system. Based on the results, the overall cost was reduced slightly. This is due to the small size of the test system, which caused the battery system to be small as well. However, if the proposed method is applied to a larger system, the total cost can be greatly reduced. Future research will concentrate on scaling up the proposed method and comparing it to other current battery technologies.

Author Contributions: Conceptualization, P.W., W.P., B.M. and B.H.; methodology, P.W. and T.B.; software P.W. and T.B.; validation, P.W., T.B., W.P., B.M. and B.H.; formal analysis, P.W., T.B., P.B., W.P., B.M. and B.H.; investigate T.B. and B.M.; data curation, T.B. and P.B.; writing—original draft preparation, P.W. and T.B.; writing—review and editing, T.B., P.B., W.P., B.M. and B.H.; supervision, B.M.; funding acquisition, B.M. All authors have read and agreed to the published version of the manuscript.

Funding: This research was funded by Suranaree University of Technology, Thailand (kittibundit-2559-3).

Institutional Review Board Statement: Not applicable.

Informed Consent Statement: Not applicable.

Conflicts of Interest: The authors declare no conflict of interest.

Abbreviations

The following abbreviations are used in this manuscript:

BESS	Battery Energy Storage System
c_1, c_2	Acceleration factors
$C_{initial}$	Initial cost
C_{om}	Fixed operation and maintenance cost
C_{re}	Replacement cost
CTF	Cycles to failure
C_{total}	Total cost
d	Discount rate
DGs	Distributed generation system
DOD	Depth of discharge
E_B	Battery energy
$E_{B, rated}$	Battery capacity
$E_{B, Orated}$	Battery's oversize energy
$E_{throughput}$	Battery throughput corresponding to a specified DOD
$E_{throughput, avg}$	Average battery throughput
g_{best}	The best global solution
G_c	The solar irradiance on the operating time
G_{STC}	The solar irradiance on the standard test condition (STC) (1000w/m ²)
i	Particle index
ite_{max}	Maximum iteration
k_c	Temperature coefficient
k	Discrete time index
$k_{B, om}$	The operation and maintenance cost set to 5% of the initial cost (\$/kWh/year)
$k_{BE, initial}$	The BESS initial cost per energy (\$/kWh)
$k_{BP, initial}$	The BESS initial cost per power (\$/kW)
L_B	BESS lifetime
L_{life}	Life loss
LPSP	Loss of power supply probability
n	Number of particles in the swarm
NPVC	Net present value of cost
NPV	Net present value
NR_B	Number of BESS replacement throughput the project
p_{best}	Personal best solution
P_B	Output power limit of BESS
$P_{B, ch}, P_{B, d}$	Charging and discharging power of BESS
$P_{B, required}$	BESS's required power
$P_{B, rated}$	BESS's rated power
$P_{B, ch}^{max}, P_{B, d}^{max}$	Upper limits of charging and discharging power of BESS
P_{PV}	Output power of PV system
$P_{rated-wt}$	Rated output power of WT

P_{STC}	Rated output power at standard test condition
PV	Photovoltaic
P_{WT}	Output power of WT
q_B	Adjusting factor
r_1, r_2	Random number [0, 1]
SOC	State of charge
T_C	The PV temperature on the operating time
USW	Uniform series presents the worth factor
v	Wind speed (m/s)
v_i	Velocity of the particle i
v_{ci}, v_r, v_{co}	Cut-in speed, rated speed and cut-off speed of WT
w	Inertia factor
W_{SOC}	Weight factor
x	Position of particle i
β	Battery's self discharge rate
$\eta_{B,chr}, \eta_{B,d}$	Charging and discharging efficiency of BESS

References

- Momoh, J.A. *Smart Grid: Fundamentals of Design and Analysis*; John Wiley & Sons: Hoboken, NJ, USA, 2012; Volume 63.
- Pinthurat, W.; Hredzak, B. Distributed Control Strategy of Single-Phase Battery Systems for Compensation of Unbalanced Active Powers in a Three-Phase Four-Wire Microgrid. *Energies* **2021**, *14*, 8287. [\[CrossRef\]](#)
- Annathurai, V.; Gan, C.K.; Ibrahim, K.A.; Baharin, K.A.; Ghani, M. A review on the impact of distributed energy resources uncertainty on distribution networks. *Int. Rev. Electr. Eng.* **2016**, *11*, 420. [\[CrossRef\]](#)
- Boonraksa, T.; Boonraksa, P.; Marungsri, B. Optimal capacitor location and sizing for reducing the power loss on the power distribution systems due to the dynamic load of the electric buses charging system using the artificial bee colony algorithm. *J. Electr. Eng. Technol.* **2021**, *16*, 1821–1831. [\[CrossRef\]](#)
- Hatziargyriou, N. *Microgrids: Architectures and Control*; John Wiley & Sons: Hoboken, NJ, USA, 2014.
- Chen, H.; Gao, L.; Zhang, Z.; Li, H. Optimal Energy Management Strategy for an Islanded Microgrid with Hybrid Energy Storage. *J. Electr. Eng. Technol.* **2021**, *16*, 1313–1325. [\[CrossRef\]](#)
- Chalise, S.; Sternhagen, J.; Hansen, T.M.; Tonkoski, R. Energy management of remote microgrids considering battery lifetime. *Electr. J.* **2016**, *29*, 1–10.
- Pinthurat, W.; Hredzak, B.; Konstantinou, G.; Fletcher, J. Techniques for compensation of unbalanced conditions in LV distribution networks with integrated renewable generation: An overview. *Electr. Power Syst. Res.* **2023**, *214*, 108932. [\[CrossRef\]](#)
- Gao, D.W. *Energy Storage for Sustainable Microgrid*; Academic Press: Cambridge, MA, USA, 2015.
- Elbaz, A.; Guner, M.T. Multi-objective optimization method for proper configuration of grid-connected PV-wind hybrid system in terms of ecological effects, outlay, and reliability. *J. Electr. Eng. Technol.* **2021**, *16*, 771–782. [\[CrossRef\]](#)
- Sansa, I.; Belaaj, N.M.; Villafafilla, R. Optimal sizing design of an isolated micro grid keeping the longest battery lifetime. In Proceedings of the 2017 International Conference on Green Energy Conversion Systems (GECS), Hammamet, Tunisia, 23–25 March 2017; pp. 1–8.
- Falai, A.; Giuliacci, T.A.; Misul, D.A.; Anselma, P.G. Reducing the Computational Cost for Artificial Intelligence-Based Battery State-of-Health Estimation in Charging Events. *Batteries* **2022**, *8*, 209. [\[CrossRef\]](#)
- Iurilli, P.; Brivio, C.; Carrillo, R.E.; Wood, V. Physics-Based SoH Estimation for Li-Ion Cells. *Batteries* **2022**, *8*, 204. [\[CrossRef\]](#)
- Narayan, N.; Papakosta, T.; Vega-Garita, V.; Qin, Z.; Popovic-Gerber, J.; Bauer, P.; Zeman, M. Estimating battery lifetimes in Solar Home System design using a practical modelling methodology. *Appl. Energy* **2018**, *228*, 1629–1639. [\[CrossRef\]](#)
- Jenkins, D.P.; Fletcher, J.; Kane, D. Lifetime prediction and sizing of lead–acid batteries for microgeneration storage applications. *IET Renew. Power Gener.* **2008**, *2*, 191–200.
- Zhao, B.; Zhang, X.; Chen, J.; Wang, C.; Guo, L. Operation Optimization of Standalone Microgrids Considering Lifetime Characteristics of Battery Energy Storage System. *IEEE Trans. Sustain. Energy* **2013**, *4*, 934–943. [\[CrossRef\]](#)
- Anuphapharadorn, S.; Sukchai, S.; Sirisamphanwong, C.; Ketjoy, N. Comparison the economic analysis of the battery between lithium-ion and lead-acid in PV stand-alone application. *Energy Procedia* **2014**, *56*, 352–358. [\[CrossRef\]](#)
- Kebede, A.A.; Coosemans, T.; Messagie, M.; Jemal, T.; Behabtu, H.A.; Van Mierlo, J.; Berecibar, M. Techno-economic analysis of lithium-ion and lead-acid batteries in stationary energy storage application. *J. Energy Storage* **2021**, *40*, 102748. [\[CrossRef\]](#)
- Chen, S.X.; Gooi, H.B.; Wang, M.Q. Sizing of Energy Storage for Microgrids. *IEEE Trans. Smart Grid* **2012**, *3*, 142–151. [\[CrossRef\]](#)
- Bai, L.; Li, F.; Hu, Q.; Cui, H.; Fang, X. Application of battery-supercapacitor energy storage system for smoothing wind power output: An optimal coordinated control strategy. In Proceedings of the 2016 IEEE Power and Energy Society General Meeting (PESGM), Boston, MA, USA, 17–21 July 2016; pp. 1–5.

21. Den Heeten, T.; Narayan, N.; Diehl, J.C.; Verschelling, J.; Silvester, S.; Popovic-Gerber, J.; Bauer, P.; Zeman, M. Understanding the present and the future electricity needs: Consequences for design of future Solar Home Systems for off-grid rural electrification. In Proceedings of the 2017 International Conference on the Domestic Use of Energy (DUE), Cape Town, South Africa, 4–5 April 2017; pp. 8–15.
22. Narayan, N.; Popovic, J.; Diehl, J.C.; Silvester, S.; Bauer, P.; Zeman, M. Developing for developing nations: Exploring an affordable solar home system design. In Proceedings of the 2016 IEEE Global Humanitarian Technology Conference (GHTC), Seattle, WA, USA, 13–16 October 2016; pp. 474–480.
23. Liu, C.; Wang, X.; Wu, X.; Guo, J. Economic scheduling model of microgrid considering the lifetime of batteries. *IET Gener. Transm. Distrib.* **2017**, *11*, 759–767. [[CrossRef](#)]
24. Xtender, S. Sun Xtender® PVX-2580L Solar Battery Specifications. Available online: <http://www.sunxtender.com/solarbattery.php?id=11> (accessed on 3 November 2022).
25. Kennedy, J.; Eberhart, R. Particle swarm optimization. In Proceedings of the ICNN'95-International Conference on Neural Networks, Perth, Australia, 27 November–1 December 1995; Volume 4, pp. 1942–1948.
26. Liu, H.; Ji, Y.; Zhuang, H.; Wu, H. Multi-objective dynamic economic dispatch of microgrid systems including vehicle-to-grid. *Energies* **2015**, *8*, 4476–4495. [[CrossRef](#)]
27. Sreenivasan, G. Solution of dynamic economic load dispatch (DELD) problem with valve point loading effects and ramp rate limits using PSO. *Int. J. Electr. Comput. Eng.* **2011**, *1*, 59. [[CrossRef](#)]
28. Dhayalini, K.; Sathiyamoorthy, S.; Rajan, C.A. Particle Swarm Optimization Technique for the Coordination of Optimal Wind and Thermal Generation Dispatch. *Int. Rev. Electr. Eng.* **2013**, *8*, 1843–1849.
29. Shi, Y.; Eberhart, R.C. Parameter selection in particle swarm optimization. In Proceedings of the International Conference on Evolutionary Programming, San Diego, CA, USA, 25–27 March 1998; Springer: Berlin/Heidelberg, Germany, 1998; pp. 591–600.
30. Birge, B. PSOT—a particle swarm optimization toolbox for use with Matlab. In Proceedings of the 2003 IEEE Swarm Intelligence Symposium. SIS'03 (Cat. No. 03EX706), Indianapolis, IN, USA, 26 April 2003; pp. 182–186.
31. Homer Software. Available online: https://www.homerenergy.com/products/pro/index.html?fbclid=IwAR3mBIFJhn92zNB5JFMnuw96avfNlx1WH_3Px5DsVxO6RlxScLq_kuxcwU8 (accessed on 20 January 2018).
32. Nguyen, C.L.; Lee, H.H. An optimal hybrid supercapacitor and battery energy storage system in wind power application. In Proceedings of the IECON 2015-41st Annual Conference of the IEEE Industrial Electronics Society, Yokohama, Japan, 9–12 November 2015; pp. 003010–003015.
33. Microgrid, S. The Advantage, and Cost of Lead-Acid and Li-Ion. Available online: <https://medium.com/solar-microgrid/battery-showdown-lead-acid-vs-lithium-ion-1d37a1998287> (accessed on 3 November 2022).
34. Sivaram, A. Cost Comparison of Battery Technology. Available online: <https://saurorja.org/2011/08/30/lead-acid-is-the-cheapest-battery-conditions-apply/> (accessed on 3 November 2022).
35. Ren, M.; Mitchell, C.R.; Mo, W. Managing residential solar photovoltaic-battery systems for grid and life cycle economic and environmental co-benefits under time-of-use rate design. *Conserv. Recycl.* **2021**, *169*, 105527. [[CrossRef](#)]

Disclaimer/Publisher's Note: The statements, opinions and data contained in all publications are solely those of the individual author(s) and contributor(s) and not of MDPI and/or the editor(s). MDPI and/or the editor(s) disclaim responsibility for any injury to people or property resulting from any ideas, methods, instructions or products referred to in the content.